Microphone Array Measurements of Concert Grand Piano Soundboards in Different Stages of Production

Niko Plath, Florian Pfeifle, Christian Koehn, Rolf Bader
Institute of Systematic Musicology, University of Hamburg
niko.plath@uni-hamburg.de

Abstract

A series of measurements is taken on two concert grand pianos in seven successive stages of production, starting with the glue-laminated soundboard planks and ending with the completely assembled piano in concert tuned state. Due to the large size of the soundboard as well as its irregular shape, measuring deflection shapes is a nontrivial task. Common measurement tools such as piezoelectric accelerometers can affect the acoustic vibrations of the soundboard due to the added mass. To this end, a noninvasive microphone array method is utilized for the present work. The array consists of 105 microphones successively placed parallel to the soundboard, resulting in a total number of 1289 microphones covering the complete surface. The Soundboard is excited using an acoustic vibrator at 15 positions associated with string termination points on the bass and main bridge. Impulse responses are obtained using the SineSweep technique. The measured sound pressure can be back-propagated to the radiating soundboard surface using a minimum energy method. Based on the measured vibrational and acoustical data a set of signal features is derived which cover direct physical behavior (e.g. driving point mobility, damping, radiation efficiency) as well as perceptive parameters (e.g. attack time, spectral centroid). This work approaches the influence of different production steps on the angle dependent bending wave velocity of the soundboard. The empirical findings will contribute to a software tool (based on a real time physical model) to help piano makers estimate the impact of design changes on the generated sound.

Measurements

A series of measurements is taken on two concert grand pianos in seven different stages of production, starting with the glue-laminated soundboard strips and ending with the completely assembled piano in concert tuned state. For all mentioned stages the piano components are temporarily taken out of the production process:

Production Stages

1. blank soundboard (glue-laminated strips of *sitka spruce*)
2. after the ribs have been attached
3. after the bridge has been attached
4. after the ribs have been notched
5. after the soundboard has been glued to the rim
6. after application of the iron frame and stringing
7. after regulation, voicing and tuning - concert tuned state

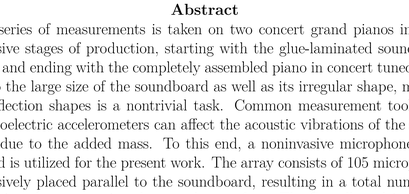

Figure 1: Experimental arrangement (left). The microphone array is situated in position 3 of 18. The shaker is situated at input position 4. A graphical representation displays coverage of the soundboard with approx. 1300 microphones (right).

Setup

- Anechoic chamber, 105 microphones (48 kHz, 24 bit).
- 18 x 105 = 1890 microphones, 1289 cover the soundboard surface (see Figure 1).
- Acoustic vibration exciter, force- and acceleration sensors at driving points.
- 15 driving points corresponding to string termination points on the bridge.

Analysis

Impulse Responses

- SineSweep technique proposed by Farina (2000), utilized for soundboard measurements by Ege (2009):
- Excitation signal: $f(t) = \sin\left[\frac{T\omega_1}{\ln(\frac{\omega_2}{\omega_1})}\left(\exp^{\frac{t}{T}\ln(\frac{\omega_1}{\omega_2})} - 1\right)\right]$
- $\omega_1 = 2\pi * 1$ (rad/s), $\omega_2 = 2\pi * 24000$ (rad/s), $T = 24$ (s)
- Deconvolution of the impulse response by linearly convolving the measured output $y(t)$ with the inverse filter $f^{-1}(t)$: $h(t) = y(t) \otimes f^{-1}(t)$

Back Propagation

- Minimum energy method proposed by Bader (2014):
- Assumption: Sum of radiating points on the surface. They may not be perfect monopoles but have a directivity normal to the surface.
- pressure in the free field $p^j = \sum_{i=1}^{N} R_{ij} p^i$
- Free-field Green´s function $R_{ij} = \frac{1}{\Gamma^{ij}} e^{ikr^{ij}}$
- Amplitude attenuation $\Gamma^{ij}(\alpha) = r^{ij}\left[1 + \alpha(1 - \beta^{ij})\right]$

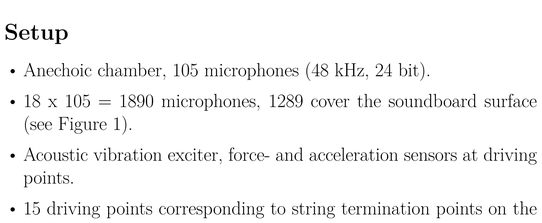

Figure 2: Magnitude of deflection for the first three soundboard resonances. Black dots depict driving point positions. (a) PROD 2 / POS 3, (b) PROD 4 / POS 1, (c) PROD 5 / POS 1, (d) PROD 6 / POS 10.

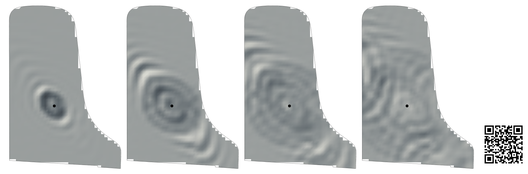

Figure 3: Shape of bending wave distribution. PROD 1, POS 9, 0.5 ms intervals (use QR code for animation).

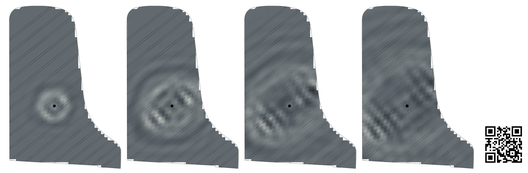

Figure 4: Shape of bending wave distribution. PROD 2, POS 9, 0.5 ms intervals (use QR code for animation).

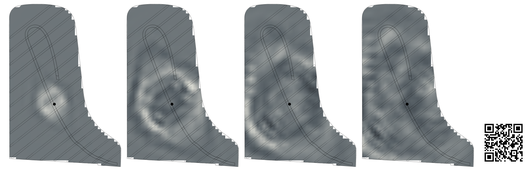

Figure 5: Shape of bending wave distribution. PROD 3, POS 9, 0.5 ms intervals (use QR code for animation).

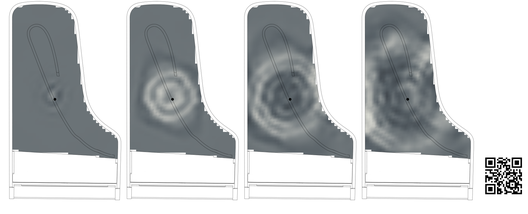

Figure 6: Shape of bending wave distribution. PROD 5, POS 9, 0.5 ms intervals (use QR code for animation).

Results

By utilizing the presented method the development of dynamic properties through the production process can be described. Figure 2 shows operating deflection shapes of the soundboard driven at resonance peaks (a) 15 Hz, (b) 27 Hz, (c) 114 Hz and (d) 98 Hz in four different stages of production.

Impact of construction steps on average angle dependent flexural wave velocity are presented: Figure 3 shows propagation of bending waves on the soundboard in first production stage. Time intervals between the pictures are .5 ms. Directivity dependence of bending wave velocity is observable, the propagation in grain direction is much faster than normal to grain. After 1.5 ms first reflections appear at the soundboard boundaries. Stiffening the soundboard normal to grain direction, by attaching the ribs, compensates the orthotropic behavior (see Figure 4). Application of the bridge increases the velocity mismatch; the bending wave propagation seems to be guided along the bridge (see Figure 5). Figure 6 shows the propagation of bending waves after the soundboard has been glued to the rim: direction dependence is mostly gone. Figure 7 shows the ratio of in grain (solid) and normal to grain (dashed) average bending wave velocity per production stage. From production stage 1 to 2 the decrease of directivity dependence is observable. Note the fact that attaching the ribs not only increases velocity normal to grain but also decreases velocity in grain direction. Application of the bridge (in grain direction for most of its length) again increases directivity dependence. Changing the boundary conditions (from production stage 4 to 5) decreases overall bending wave velocity.

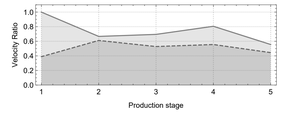

Figure 7: Ratio of average bending wave velocity in grain direction (solid) and normal to grain direction (dashed) per production stage.

Acknowledgements

The authors acknowledge support by the *Deutsche Forschungsgemeinchaft (DFG)*.

References

Bader, Rolf (2014). "Microphone Array". In: *Springer Handbook of Acoustics*. Ed. by Thomas D. Rossing. Springer New York. Chap. Microphone, pp. 1179–1207.

Ege, Kerem (2009). "La table d'harmonie du piano-Études modales en basses et moyennes fréquences". PhD thesis.

Farina, Angelo (2000). "Simultaneous measurement of impulse response and distortion with a swept-sine technique". In: *Audio Engineering Society Convention 108*, pp. 1–24.